Conserved genetic determinant of motor organ identity in *Medicago truncatula* and related legumes

Jianghua Chen[a], Carol Moreau[b], Yu Liu[a], Masayoshi Kawaguchi[c], Julie Hofer[b,d], Noel Ellis[b,d], and Rujin Chen[a,1]

[a]Plant Biology Division, Samuel Roberts Noble Foundation, Ardmore, OK 73401; [b]Department of Crop Genetics, The John Innes Centre, Colney, Norwich NR4 7UH, United Kingdom; [c]Division of Symbiotic Systems, National Institute for Basic Biology, Myodaiji-cho, Okazaki 444-8585, Japan; and [d]Institute of Biological, Environmental and Rural Sciences, Aberystwyth University, Aberystwyth, Ceredigion SY23 3EE, United Kingdom

Edited by Sarah Hake, University of California, Berkeley, CA, and approved May 11, 2012 (received for review March 16, 2012)

Plants exhibit various kinds of movements that have fascinated scientists and the public for centuries. Physiological studies in plants with the so-called motor organ or pulvinus suggest that cells at opposite sides of the pulvinus mediate leaf or leaflet movements by swelling and shrinking. How motor organ identity is determined is unknown. Using a genetic approach, we isolated a mutant designated *elongated petiolule1* (*elp1*) from *Medicago truncatula* that fails to fold its leaflets in the dark due to loss of motor organs. Map-based cloning indicated that *ELP1* encodes a putative plant-specific LOB domain transcription factor. RNA in situ analysis revealed that *ELP1* is expressed in primordial cells that give rise to the motor organ. Ectopic expression of *ELP1* resulted in dwarf plants with petioles and rachises reduced in length, and the epidermal cells gained characteristics of motor organ epidermal cells. By identifying *ELP1* orthologs from other legume species, namely pea (*Pisum sativum*) and *Lotus japonicus*, we show that this motor organ identity is regulated by a conserved molecular mechanism.

leaf movements | nyctinastic plants | lateral organ boundaries domain genes | *Apulvinic* | *Sleepless*

Land plants are sessile organisms; once they have germinated, they are rooted in soil. To prevail with their immobile lifestyle, plants have evolved various mechanisms to optimize their development in response to ever-changing external, environmental signals. Plant responses to the environment include tropic responses, such as phototropism, gravitropism, and heliotropism, that depend on the direction of external signals, and nastic responses, such as sleep movements of leaves in nyctinastic plants (1, 2), that are independent of the direction of external signals. In general, these responses are slow and can be best documented by time-lapse photography (3). In other cases, however, these can be very fast; for example, the sensitive plant (*Mimosa pudica*) collapses its leaves within seconds of being touched or shaken; the carnivorous Venus flytrap (*Dionaea muscipula*) snaps shut its traps when hairs are brushed by an insect.

Plant responses to environmental cues include irreversible differential growth responses initiating from signal perception and transduction and resulting in curvature responses of young tissues in shoots and roots (4–6), as well as reversible movements involving a specialized structure—a motor organ or pulvinus—located at the base of a leaf or leaflet (7). The motor organ-driven leaf or leaflet movement observed predominantly in species of Leguminosae (Fabaceae) and Oxalidaceae families involves flattening leaves or leaflets during the day and folding them at night and is known to follow a circadian rhythm (7). Changes in turgor in cells at opposite sides of the motor organ drive the leaf/leaflet movement (8–15). Although this type of leaf movement and the anatomy of motor organs have been well studied, how the identity of the motor organ is determined has remained unknown. Here we report isolation and characterization of three orthologous genes—*ELONGATED PETIOLULE1* (*ELP1*) of *Medicago truncatula*, *Apulvinic* (*Apu*) of *Pisum sativum*, and *SLEEPLESS* (*SLP*) of *Lotus japonicus*—and their role in determining motor organ identity in legumes.

Results and Discussion

Isolation and Characterization of *M. truncatula elongated petiolule1* Mutants. Classical mutants with altered motor organ identity are known in pea (*P. sativum*) and *L. japonicus*: that is, *apulvinic* (*apu*) and *sleepless* (*slp*), respectively (16–18). Using a forward genetic screen of fast neutron (FN)-induced mutants of the model legume *M. truncatula* (cv Jemalong A17), we isolated a mutant line that was unable to fold its leaflets in the dark in contrast to wild-type (WT) plants (Fig. S1 *A* and *B*). The mutant, *elongated petiolule1-1* (*elp1-1*), was backcrossed to the WT parent. F1 plants derived from the crosses exhibited WT phenotype, and F2 plants from self-pollination of the F1 plants exhibited segregation of WT and mutant in a ratio of 3:1 (142 WT and 48 mutants; $P < 0.01$; Table S1), indicating that *elp1-1* was caused by a single recessive mutation.

Phenotypic analysis indicated that the pulvinus, a short cylindrical structure with a radial symmetry located at the base of WT leaflets (Fig. 1*A*; arrows; Fig. S1*C*) is absent from both unifoliate and trifoliate leaves of the *elp1-1* mutant (Fig. 1*B*, asterisks; Fig. S1*D*). This phenotype is apparent in longitudinal sections, which show that isodiametric pulvinus cells in WT plants are replaced by rachis- or petiole-like cells in the *elp1-1* mutant, with an average cortical cell length about sixfold longer and an average cell width about 64% wider than in the pulvinus of WT plants (Fig. 1 *C* and *D*; Fig. S2). The pulvinus in WT plants exhibits a radial symmetry as indicated by the presence of a central vascular bundle surrounded by nearly identical cortical cells (19) (Fig. 1*E*). In the *elp1-1* mutant, this organ is replaced by one similar to the rachis or petiole, exhibiting an adaxial–abaxial polarity as shown by the presence of one large vascular bundle on the abaxial side and two small vascular bundles and larger cortical cells on the adaxial side (Fig. 1*F*).

Scanning electron microscope (SEM) images show that the surface of pulvinus epidermal cells is highly convoluted. Patches of longitudinal folds are regularly interspersed with similar latitudinal folds, giving the appearance of knitted wool (Fig. 1 *G–I*). By contrast, no such cell surface modifications are observed in the *elp1-1* mutant (Fig. 1 *J–L*).

Author contributions: J.C., C.M., N.E., and R.C. designed research; J.C., C.M., and Y.L. performed research; M.K. contributed new reagents/analytic tools; J.C., C.M., J.H., N.E., and R.C. analyzed data; and J.C. and R.C. wrote the paper.

The authors declare no conflict of interest.

This article is a PNAS Direct Submission.

Data deposition: The sequences reported in this paper have been deposited in the GenBank database [accession nos. JQ653161 (ELP1), JQ653162 (SLP), JQ653163 (Apu), JQ653164 (Glyma06g18860), and JQ653165 (Glyma04g36080)].

See Commentary on page 11474.

[1]To whom correspondence should be addressed. E-mail: rchen@noble.org.

This article contains supporting information online at www.pnas.org/lookup/suppl/doi:10.1073/pnas.1204566109/-/DCSupplemental.

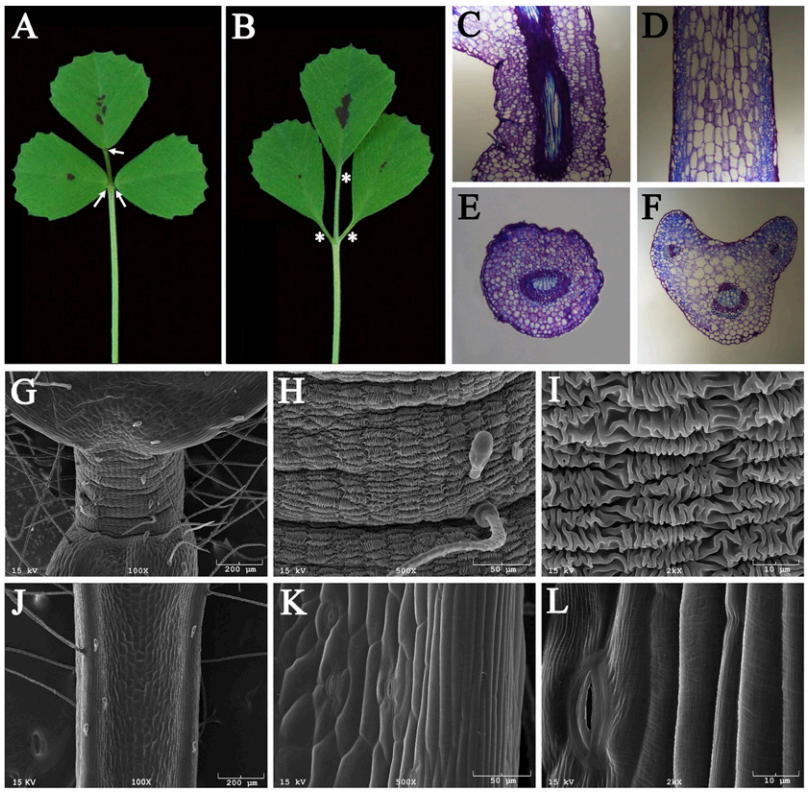

Fig. 1. *M. truncatula elongated petiolule 1* (*elp1*) mutant lacks motor organs. (*A* and *B*) Morphologies of trifoliate leaves of wild type (*A*) and the *elp1-1* mutant (*B*). Arrows indicate pulvini in *A* and asterisks the equivalent positions in *B*. (*C* and *D*) Longitudinal sections of a pulvinus of WT (*C*) or the replacement organ of the *elp1* mutant (*D*). (*E* and *F*) Cross sections of a pulvinus of WT (*E*) or the replacement organ of the *elp1* mutant (*F*). (*G*–*L*) Scanning electron microscope images of a pulvinus of WT (*G*–*I*) or the replacement organ of the *elp1* mutant (*J*–*L*) with different magnifications.

Molecular Cloning of the *M. truncatula ELP1* Gene. Using a map-based approach, we positioned the *ELP1* locus on the lower arm of chromosome 3 flanked by three simple sequence repeat (SSR) markers (AC151725-1, CR538722-1, and AC147538-1) and tightly linked to a fourth SSR marker (h2-9b13a) (Fig. 2*A*; Tables S1 and S2). Fine genetic mapping using a mapping population of 2,088 F2 plants and the additional markers, CT573365-92k, h2-17f20a, and CT954236-86.6k, further defined the *elp1* map position (Fig. 2 *B* and *C*; Tables S1 and S2). To identify the *ELP1* gene, we screened a *Tnt1* retrotransposon insertion mutant collection of *M. truncatula* (cv R108) (20, 21) and isolated additional mutant lines that resemble the *elp1-1* mutant (Table S3). F1 plants derived from crosses between *elp1-1* and additional lines exhibited the same phenotype as the single mutants, confirming that they are allelic to each other. Flanking sequence analysis indicated that *elp1-2*, *elp1-4*, and *elp1-5* alleles carry a *Tnt1* retrotransposon inserted between 178 and 179, 37 and 38, and 130 and 131 bases, respectively, and that the *elp1-3* allele carries a native retrotransposon, *MERE1* (22), between bases 251 and 252 downstream of the translation initiation codon of ORF4 (Fig. 2 *C* and *D*; Fig. S3). We sequenced ORF4 from the *elp1-1* allele and identified a single-nucleotide insertion between bases 53 and 54, which would result in a frameshift and premature termination of the encoded protein (Fig. 2*D*; Fig. S3).

The *ELP1*-coding sequence, under control of the constitutive cauliflower mosaic virus 35S promoter and translationally fused to green fluorescent protein (*35S:GFP-ELP1*), complemented the *elp1-3* mutation in stable transformants. In two of five independent transgenic lines that were generated, the *elp1-3* mutant phenotype was completely rescued without pleiotropic effects (Fig. 2 *E*–*H*). Reverse transcription (RT)-PCR analysis indicated that the *ELP1* gene was expressed in these transgenic plants but not in the *elp1-3* mutant (Fig. 2*I*). The remaining three transgenic lines were severely dwarfed, but the pulvinus was restored in these lines. Collectively, these data indicate that ORF4 corresponds to the *ELP1* gene.

Basic Local Alignment Search Tool (BLAST) analysis of the National Center for Biotechnology Information protein database identified ELP1 homologous sequences from closely and distantly related species including soybean (*Glycine max*), *L. japonicus*, *Arabidopsis thaliana*, and maize (*Zea mays*). In *Arabidopsis*, LOB, the founding member of the large plant-specific lateral organ boundaries domain (LBD) transcription factor family (23–27), is most similar to ELP1. In maize, two closely related homologs are ramosa 2 (ra2) and indeterminate gametophyte 1 (ig1), which are closely related to the *Arabidopsis* LOB and LBD6/ASYMMETRIC LEAVES2 (AS2), respectively (28–30). Using RT-PCR and degenerate *ELP1* primers, we amplified cDNA sequences from pea (*P. sativum*) and *L. japonicus*. Phylogenetic analysis grouped the legume ELP1 homologous sequences together (Fig. 2*J*; Fig. S4). Amino acid sequence alignments indicate that the legume ELP1 sequences share a high degree of amino acid sequence similarities in the N-terminal LOB domain with closely related sequences from *Arabidopsis* and maize, but these sequences are highly divergent from each other in the C-terminal variable region as previously reported for the LBD sequences (26) (Fig. 2*K*; Fig. S5).

RNA in situ hybridization shows that *ELP1* transcripts were detected in a small number of cells in the basal (proximal) region of emerging leaflet primordia as early as P3 (plastochron 3), before the development of the pulvinus (Fig. 3 *A* and *B*). *ELP1* transcripts were present in the basal region of developing leaflet primordia until at least the P6 stage when the pulvinus was first apparent. RNA in situ hybridization results further showed that *ELP1* was not detectably expressed in the shoot apical meristem and laminar tissues (Fig. 3 *A* and *B*). A negative control hybridized with a sense probe did not detect any signals (Fig. 3*C*).

To examine the subcellular localization of the ELP1 protein, we expressed *35S:GFP-ELP1* in onion epidermal cells. The results show that the fusion protein was localized to the nucleus, supporting its role as a putative transcription factor (Fig. 3 *D*–*F*).

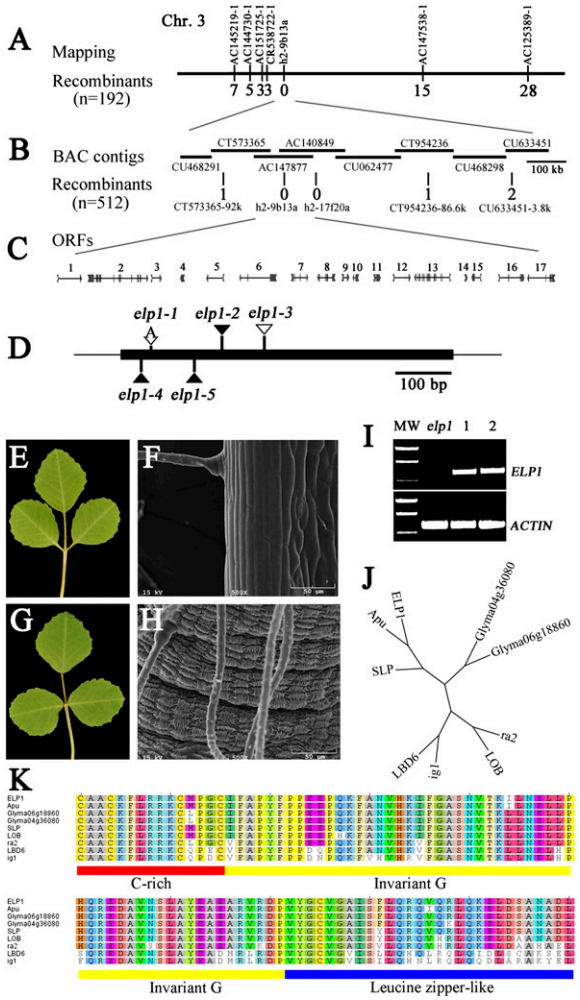

Fig. 2. Map-based cloning, genetic complementation, and phylogenetic analysis of the *M. truncatula ELP1* gene. (*A*) The *elp1* locus was mapped to the lower arm of chromosome 3 and tightly linked to the SSR marker h2-9b13a. (*B*) Fine genetic mapping using a large F2 population further narrowed the *elp1* map position. Horizontal lines represent BAC contigs in the mapped region. The number of recombinants with respect to *elp1* is provided below each marker in *A* and *B*. (*C*) Predicted genes and gene structures in the mapped region. (*D*) Mutation sites in ORF4 identified in *elp1* mutant alleles. (*E–H*) Genetic complementation of *elp1-3*. Shown are representative *elp1-3* mutant trifoliate leaf (*E*) and SEM image of the base of a leaflet (*F*) and representative trifoliate leaf (*G*) and SEM image of the base of a leaflet (*H*) of the *elp1-3* mutant transformed with *35S:GFP-ELP1*. (*I*) RT-PCR analysis of *ELP1* expression. MW, molecular weight markers; *elp1*, *elp1–3*; lanes 1 and 2, two independent transgenic lines in which *ELP1* gene expression was restored. *M. truncatula ACTIN* gene was used as a loading control. (*J*) Phylogenetic relationship analysis of ELP1 and its closely related homologs, Apu from pea (*P. sativum*), SLP from *L. japonicus*, LOB (At5g63090), and LBD6/AS2 (At1g65620) from *A. thaliana*, Glyma04g36080 and Glyma06g18860 from soybean (*G. max*), and ra2 and indeterminate ig1 from maize (*Zea mays*). (*K*) Amino acid sequence alignments of N-terminal LOB domains of ELP1 and its homologs. The underlined LOB domain includes cysteine (C)-rich (red), invariant glycine (G; yellow), and leucine-zipper–like (blue) motifs.

Molecular Cloning of Pea *Apu* and *L. japonicus SLP*. To investigate the genetic control of motor organ identity in other species, we characterized causative mutations in *apu* mutants of pea (*P. sativum*) and *slp* mutants of *L. japonicus* (16–18) (Fig. 4 *A* and *I*). SEM images show that the pea pulvinus has cell-surface convolutions similar to those of *M. truncatula* and that the *apu* mutants lack these structures (Fig. 4 *B–G*). The *apu* mutation was previously mapped to pea linkage group III (PsLgIII) (17, 18, 31) in a position syntenic to the *ELP1* region (32). We analyzed five *apu* mutants generated by FN mutagenesis and 18 *apu* mutants generated by ethylmethane sulfonate (EMS) mutagenesis or natural variation (Table S3). Using primers based on *L. japonicus LBD* genes that are expressed at the base of leaves (27), we identified sequences that are deleted in *apu* FN mutants. PCR experiments with four *apu* alleles failed to amplify any part of the gene that is homologous to *ELP1*, consistent with complete deletions. One *apu* FN mutant carried a deletion upstream of the coding region of the same gene, resulting in greatly reduced gene expression as shown by quantitative RT-PCR (Fig. 4*H*; Fig. S6). Four *apu* alleles from the John Innes (JI) *Pisum* germplasm collection carry point mutations at different positions in the coding region of the pea *Apu* gene (Fig. 4*H*; Fig. S5); 14 *apu* mutants from the US Department of Agriculture Marx collection all carry the same point mutation in the *Apu* gene as the JI1349 allele (Table S3; Fig. S5). In summary, two point mutations (T152A and A278C) are missense mutations that would result in amino acid changes (V51E and Q93P) in the highly conserved LOB domain, and two (C314 A and C397T) are nonsense mutations (S105* and Q133*) that would result in the loss of the C-terminal half of the encoded protein (Fig. S5).

To extend our genetic analysis, a pea TILLING mutant collection (33) was screened. This identified one line (T3593) carrying a missense mutation (C172T) that exhibits the *apu* mutant phenotype, indicating that the L58F change in the conserved LOB domain also disrupts the protein function (Fig. 4*H*; Fig. S5). *Apu* cDNA sequence can be amplified using RT-PCR and degenerate *ELP1* primers (Fig. 2 *J* and *K*). These results collectively indicate that *Apu* and *ELP1* are functional orthologs.

The *L. japonicus slp* mutant was originally isolated from an EMS-induced mutant collection for its inability to close leaflets in the dark (16). Consistent with previous studies, SEM image analysis indicates that the *slp* mutant lacks the pulvinus as do the *M. truncatula elp1* and the pea *apu* mutants (Fig. 4 *J–M*). PCR amplification with degenerate *ELP1* primers and sequence analysis of WT (Gifu B-129) and the *slp* mutant show that the *slp* mutant carries a missense mutation (C229T), which would result in an R77C change in the conserved LOB domain of a *L. japonicus LBD* gene (Fig. 4*N*; Fig. S5). We backcrossed the *slp1* mutant to the WT plant and generated a segregating F2 population (Table S1). The C229T mutation cosegregated with the *slp* mutant phenotype in the F2 population. Taken together, these results support our conclusion that *SLP* corresponds to the *Lotus ELP1* ortholog.

Ectopic Expression of *ELP1* in *M. truncatula*. Our results demonstrate a role of *ELP1* in the development of the motor organ. To further test its role, we introduced the *35S:GFP-ELP1* construct into WT plants (*M. truncatula* cv. R108) and generated six independent transgenic lines. All six transgenic lines exhibited a severe dwarf phenotype but were fertile (Fig. 5 *A–C*). In the *elp1-3* mutant background, three of five independent transgenic lines that were generated with the same construct also exhibited a similar dwarf phenotype. Quantitative RT-PCR analysis of two representative lines showed that the expression level of *ELP1* was increased more than 40-fold (Fig. 5*D*). The average length of petioles and rachises was significantly reduced in the transgenic plants compared with WT plants (Fig. S7). The degree of reduction correlates with the degree of reduction in epidermal cell length in petioles and rachises of the transgenic plants compared with WT (Fig. 5*E*; Fig. S7). SEM image analysis shows that epidermal cells of both petioles and rachises of the transgenic plants undergo surface modifications resembling, to some degree, the epidermal cells of the motor organ of WT plants (Fig. 5 *F*, *J*, and *K*). In addition, surface modifications of pulvinus epidermal cells of the transgenic lines (Fig. 5*I*) were somewhat irregular compared with WT plants (Fig. 5*F*), suggesting that an

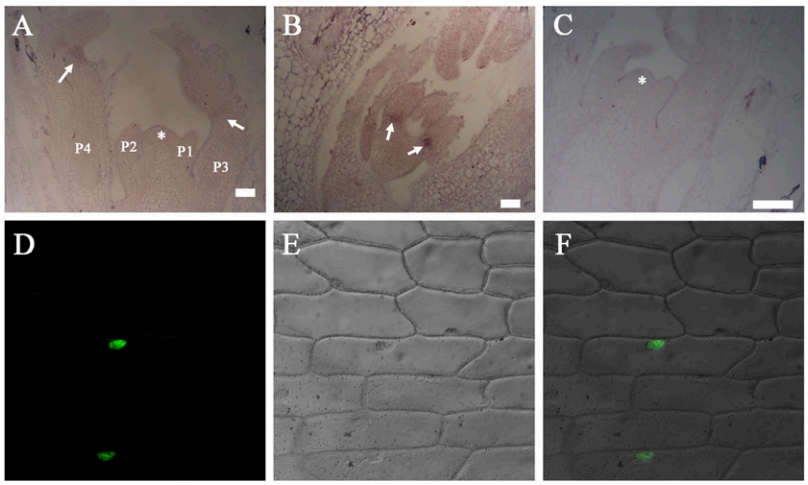

Fig. 3. RNA in situ hybridization and subcellular protein localization. (*A* and *B*) Longitudinal sections of vegetative shoot bud (*A*) and leaf primordium (*B*) showing that *ELP1* transcripts were detected in a small number of cells at the basal region of young leaflets (arrows). (*C*) No hybridization signals were detected in an adjacent section hybridized with an *ELP1* sense probe. Asterisks denote the shoot apical meristem and P represents the plastochron. (*D–F*) Nuclear localization of GFP-ELP1 fusion protein driven by the CaMV35S promoter in onion epidermal cells. Shown are a representative confocal image of the GFP signal (*D*), a Normaski image of onion epidermal cells (*E*), and an overlay of the two images (*F*).

increase in *ELP1* expression affected pulvinus epidermal cell patterning and development.

Several members of the *LBD* gene family have been shown to play important roles in developmental and metabolic processes in *Arabidopsis* and grasses (26, 28, 29, 34, 35). *Arabidopsis* plants do not have a pulvinus at the base of their leaves and no phenotypic alterations are observed in loss-of-function mutants of the *LOB* gene, yet ectopic expression of *LOB* results in severely dwarfed and sterile plants (23). Domain swapping experiments show that the LOB domain coded by *Arabidopsis ASYMMETRIC LEAF2* (*AS2*/*LBD6*) cannot be replaced by structurally related LOB domains coded by other *LBD* genes (25). This suggests that each *LBD* gene may have distinct targets in *Arabidopsis* plants. In maize, the two closely related LOB domain transcription factors, ra2 and ig1, determine the fate of stem cells in branch meristems and inflorescence architecture and in embryo sac and leaf development, respectively (28–30). In grasses including maize, a motor organ called the leaf sheath pulvinus is present at the base of a leaf sheath (7). It is involved in maintaining the vertical orientation of grass shoots and restoring it after lodging by rain, wind, or other causes. It remains to be seen whether grasses use LOB domain transcription factors in defining the leaf sheath pulvinus identity. It is noteworthy that the leaf sheath pulvinus of grasses differs from the pulvinus present in leguminous plants in that it mediates irreversible growth responses (7). Our results demonstrate a previously unidentified role of the legume *LBD* gene *ELP1* from *M. truncatula* and its orthologs, *Apu* from pea and *SLP* from *L. japonicus* in motor organ identity determination. Interestingly, in contrast to *AS2* of *Arabidopsis* and *ig1* of maize, whose function is required for the establishment of abaxial–adaxial polarity in leaves, *ELP1*/*Apu*/*SLP* function results in loss of abaxial–adaxial polarity and gain of radial symmetry in the specific context of the pulvinus. The identification of *ELP1* from *M. truncatula* and its functional orthologs from other legumes thus fills a major gap in our understanding of the genetic control of development of pulvinus, a motor organ required for leaflet movements that fascinated scientists and the public for centuries (1, 2). This further provides a unique

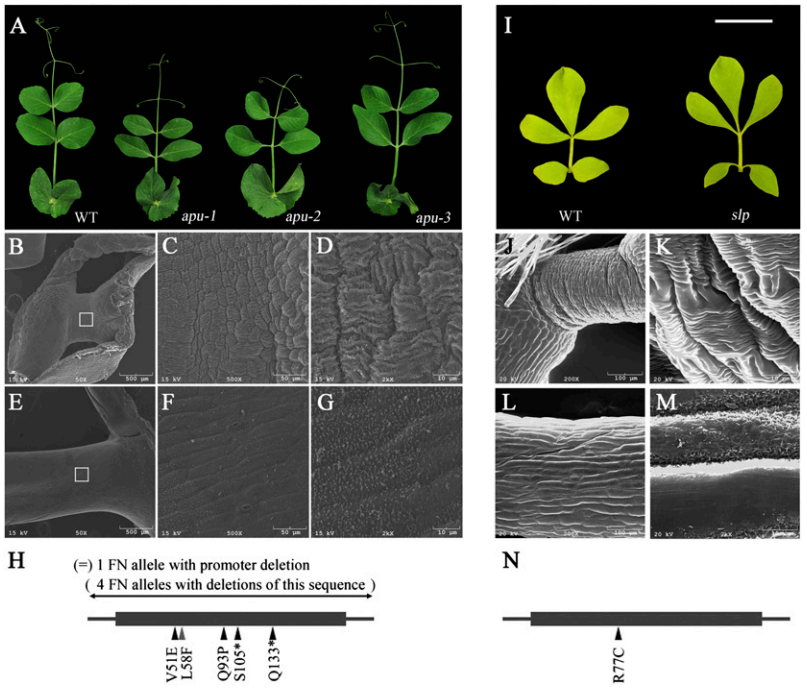

Fig. 4. Phenotypic analysis and molecular cloning of *apu* mutants of pea (*P. sativum*) and a *slp* mutant of *L. japonicus*. (*A*) Representative images of compound leaves of WT, *apu-1*, *apu-2*, and *apu-3* alleles (from left to right). (*B–G*) SEM images with different magnifications of the pulvinus of a WT plant (*B–D*) and the replacement organ of *apu-1* mutant (*E–G*). Open boxes in *B* and *E* indicate areas shown in *C* and *F*. (*H*) Different *apu* alleles and mutation sites. (*I*) Representative images of compound leaves of WT (Gifu B-129; *Left*) and *slp* mutant (*Right*). (*J–M*) SEM images of the pulvinus of a WT plant (*J* and *K*) and the replacement organ of a *slp* mutant (*L* and *M*). (*N*) The mutation site of the *slp* mutant.

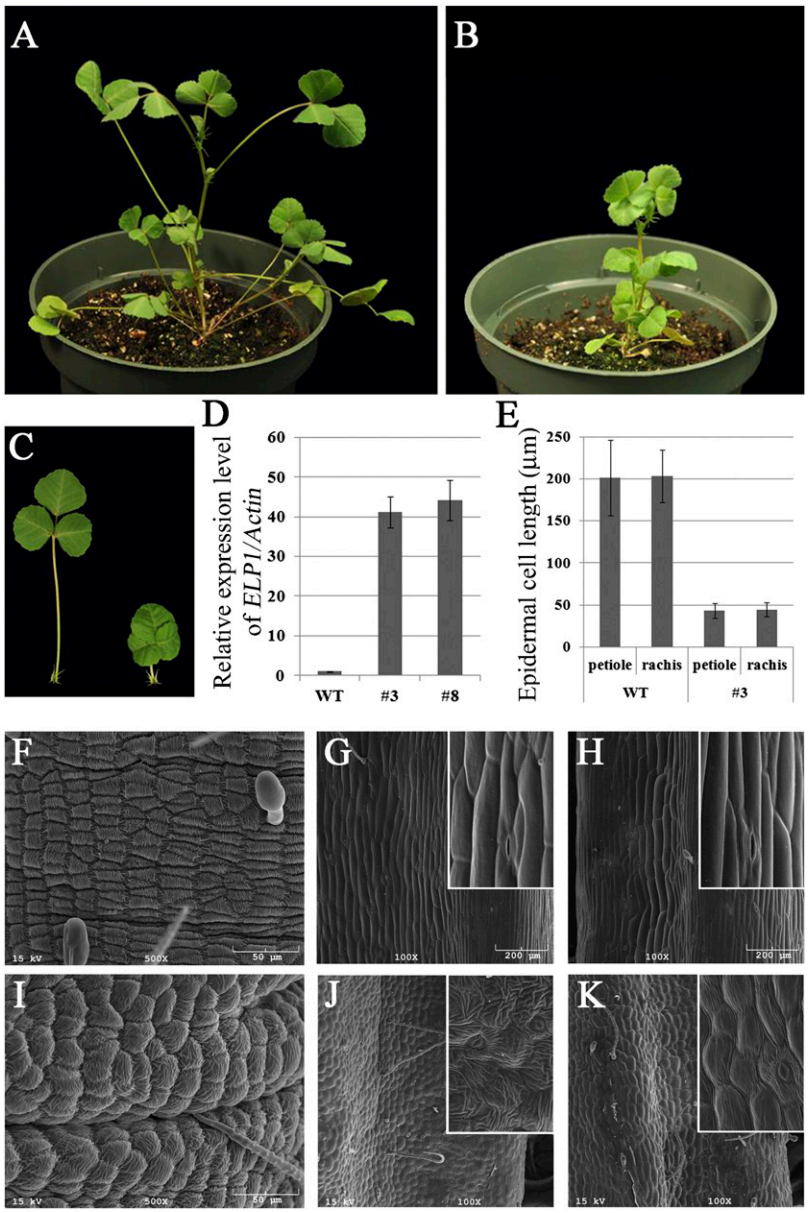

Fig. 5. Ectopic expression of *ELP1* in *M. truncatula*. (*A* and *B*) Images of 1-mo-old WT plant (cv. R108; *A*) and a transgenic plant transformed with *35S:GFP-ELP1* (*B*) showing a severe dwarf phenotype of the transgenic line. (*C*) Close-up images of trifoliate leaves of WT (*Left*) and the *35S:GFP-ELP1* line (*Right*). (*D*) Quantitative RT-PCR analysis of *ELP1* gene expression in WT and two independent *35S:GFP-ELP1* lines, 3 and 8. *ELP1* gene expression was normalized with the *M. truncatula ACTIN* gene. (*E*) Measurements of epidermal cell length of petiole and rachis in WT and the *35S:GFP-ELP1* line 3. Shown are means ± SD; $n = 60$. (*F–K*) SEM images of pulvini (*F* and *I*), petioles (*G* and *J*), rachises (*H* and *K*) of WT (*F–H*), and the *35S:GFP-ELP1* line 3 (*I–K*). *Insets* are magnified images.

opportunity to investigate the origin of motor organs during plant evolution and the regulatory mechanism that underlies the diverse motor organ-driven leaf movements seen in nature.

Materials and Methods

Plant Materials and Growth Conditions. *M. truncatula elp1* mutants were isolated from FN and *Tnt1* mutant collections as previously reported (19, 36). Pea *apu* mutants were identified from the pea germplasm collections at The John Innes Centre (http://data.jic.bbsrc.ac.uk/cgi-bin/germplasm/pisum/) and the US Department of Agriculture-Agricultural Research Service Pacific West. The *L. japonicus slp* mutant was as previously reported (16). Plants were grown in greenhouses under the following controlled conditions: 16 h/8 h day/night cycle, 150 $\mu E/m^2/s$ light intensity, 22 °C/18 °C day/night temperature, and 70% humidity.

Genetic Mapping. F2 mapping populations were generated from self-pollination of F1 plants derived from crosses between *elp1-1* mutant (cv. Jemalong A17) and a polymorphic ecotype, *M. truncatula* cv. Jemalong A20. The *ELP1* locus was mapped by bulked segregant analysis (BSA) and fine genetic mapping following procedures as previously reported (19, 36). For BSA, two bulked pools from 50 F2 mutant plants each were analyzed using 93 SSR markers distributed on the eight chromosomes (37). For fine genetic mapping, 10 SSR markers within the mapped region are used to identify recombinants within a large F2 segregation population.

SEM Analysis. SEM analysis was essentially carried out as previously described (19, 20).

Rapid amplification of cDNA ends. Annotation of genomic sequence suggests that ELP1 may harbor a conspicuous intron in the 3′ end. To empirically test this, we carried out 3′ rapid amplification of cDNA ends (RACE) experiments, using an RLM-RACE kit (Invitrogen) and following the manufacturer's instructions. The results of these experiments indicate that the ELP1 genomic sequence does not harbor any introns (Fig. S3). Primer sequences are listed in Table S2.

Phylogenetic Analysis. Phylogenetic trees were constructed using neighbor-joining, maximum parsimony, and UPGMA algorithms implemented in the MEGA software suite (38) (http://www.megasoftware.net/) with 1,000 bootstrap replications. Multiple sequences were aligned using Clustal_X (39).

Subcellular Localization. Green fluorescent protein (GFP)-coding sequence was fused in-frame to the 5′ end of the *ELP1*-coding sequence, and the fusion

construct was driven under the control of the cauliflower mosaic virus (CaMV) 35S promoter. The fusion construct was bombarded into onion epidermal cells using the Helium Biolistic Device (PDS-1000; Bio-Rad). Localization of the GFP-ELP1 fusion protein was examined using a confocal laser scanning microscope (TCS SP2 AOBS; Leica).

RNA in Situ Hybridization. RNA in situ hybridization was carried out essentially as previously described (40). *ELP1* sense and antisense probes correspond to a 264-bp 3′ sequence of *ELP1*. Ten-micrometer sections from shoot apices of 2- to 4-wk-old seedlings were processed and hybridized with digoxigenin-labeled sense and antisense probes.

Quantitative RT-PCR. Total RNA samples were isolated from plant tissues using RNeasy Plant Mini Kit (Qiagen). DNase kit (Qiagen) was used to remove genomic DNA residues. The RNA quality was determined by Nanodrop Analyzer (BioMedical Solutions). Reverse transcription and cDNA synthesis were carried out with 2 μg of total RNA, using Omniscript RT Kit (Qiagen) and oligo(dT)15 primer. Real-time RT-PCR analysis was carried out as previously described (36). Primer sequences are listed in Table S2.

Genetic Complementation. Full-length *ELP1*-coding sequence (0.579 kb) was amplified by PCR and cloned into the pENTR/D-TOPO vector (Invitrogen). After sequence verification, the insert was subcloned into the binary vector pK7WGF2 (41). The resulting plasmid was introduced into the *Agrobacterium tumefaciens* EHA105 strain, which was subsequently used to transform *M. truncatula*. Primer sequences are listed in Table S2.

Genetic Segregation Analysis of Pea *apu* and *L. japonicus slp* Mutants. *L. japonicus slp* mutant was cross-pollinated with WT (Gifu B-129). In the F2 population, WT and *slp* mutant plants segregated in a ratio of 3:1 (Table S1). PCR using degenerate *ELP1* primers and subsequent sequence analysis identified in the *L. japonicus ELP1* homolog, *SLP*, a missense mutation (C229T; R77C), which results in loss of a recognization site for the restriction enzyme Sau961 (catalog no. R0165S; New England Biolab). Sau961 enzyme digestion of a 573-bp fragment amplified by PCR from WT and the *slp* mutant results in three fragments (11, 225, and 337 bp) and two fragments (236 and 337 bp) from WT and the *slp* mutant, respectively. The C229T mutation was cosegregated with *slp* mutant plants in the F2 population.

The *apu* locus was mapped to the pea linkage group III. Using a candidate gene approach and sequence analysis of multiple alleles, we identified the pea *APU* gene. We also amplified the pea *APU* gene using PCR and degenerate *ELP1* primers. Sequence analysis of six *apu* alleles (W6-15174, W6-15175, W6-15176, W6-15190, W6-151274, and W6-15380) from the Marx collection of pea *apu* mutants (US Department of Agriculture-Agricultural Research Station Pacific West Germplasm Collection) identified the same nonsense mutation (C314A; S115*) in these lines, which is identical to the *apu-1* (JI1349) mutation. C314A mutation results in loss of the HinfI restriction site. HinfI restriction enzyme digestion of a 579-bp fragment amplified by PCR from WT and the remaining eight Marx *apu* alleles giving rise to two fragments (413 and 166 bp) and one fragment (579 bp), respectively, suggests that the remaining Marx *apu* alleles carry the same nonsense mutation as the *apu-1* allele. Primer sequences are listed in Table S2.

ACKNOWLEDGMENTS. We thank our colleagues for insightful discussions and comments on the manuscript; Preston Larson (University of Oklahoma), Shuirong Zhang, and Guangming Li for assistance with SEM analysis, plant care, and tissue culture, respectively; Kirankumar Mysore and Pascal Ratet (Gifu) for assistance with the *Medicago Tnt1* lines; Mike Ambrose (The John Innes Centre) for pea FN mutants; Marion Dalmais, Christine Le Signore, and Abdelhafid Bendahmane (Institut National de la Recherche Agronomique) for pea TILLING mutants; The John Innes Center and US Department of Agriculture-Agricultural Research Station Pacific West for pea EMS mutants and natural variants; and Jackie Kelly for editorial assistance. Funding for work done in R.C.'s laboratory was provided in part by The Samuel Roberts Noble Foundation and the National Science Foundation (DBI 0703285). Additional funding was provided by European Commission Framework Program VI Grain Legumes Integrated Project FP6-2002-FOOD-1-506223 (N.E. and J.H.) and Department for Environment, Food, and Rural Affairs Pulse Crop Genetic Improvement Network Grant AR0711 (to C.M.).

1. Koller D (2011) *The Restless Plant* (Harvard Univ Press, Cambridge, MA).
2. Darwin C (1897) *The Power of Movement in Plants* (D. Appleton and Company, New York).
3. Hangarter R (2000) *Plants-In-Motion*. Available at http://plantsinmotion.bio.indiana.edu/plantmotion/starthere.html.
4. Chen R, Guan C, Boonsirichai K, Masson PH (2002) Complex physiological and molecular processes underlying root gravitropism. *Plant Mol Biol* 49:305–317.
5. Chen R, Rosen E, Masson PH (1999) Gravitropism in higher plants. *Plant Physiol* 120:343–350.
6. Chen R, et al. (1998) The *Arabidopsis thaliana AGRAVITROPIC 1* gene encodes a component of the polar-auxin-transport efflux carrier. *Proc Natl Acad Sci USA* 95:15112–15117.
7. Satter RL, Gorton HL, Vogelmann TC (1990) *The Pulvinus: Motor Organ for Leaf Movement* (American Society of Plant Physiologists, Rockville, MD).
8. Moran N (2007) Osmoregulation of leaf motor cells. *FEBS Lett* 581:2337–2347.
9. Nakamura Y, et al. (2011) 12-Hydroxyjasmonic acid glucoside is a COI1-JAZ-independent activator of leaf-closing movement in *Samanea saman*. *Plant Physiol* 155:1226–1236.
10. Ueda M, Nakamura Y (2007) Chemical basis of plant leaf movement. *Plant Cell Physiol* 48:900–907.
11. Cote GG (1995) Signal transduction in leaf movement. *Plant Physiol* 109:729–734.
12. Moran N (1996) Membrane-delimited phosphorylation enables the activation of the outward-rectifying K channels in motor cell protoplasts of *Samanea saman*. *Plant Physiol* 111:1281–1292.
13. Kim HY, Coté GG, Crain RC (1993) Potassium channels in *Samanea saman* protoplasts controlled by phytochrome and the biological clock. *Science* 260:960–962.
14. Moran N, Fox D, Satter RL (1990) Interaction of the depolarization-activated K channel of *Samanea saman* with inorganic ions: A patch-clamp study. *Plant Physiol* 94:424–431.
15. Moran N, et al. (1988) Potassium channels in motor cells of *Samanea saman*: A patch-clamp study. *Plant Physiol* 88:643–648.
16. Kawaguchi M (2003) *SLEEPLESS*, a gene conferring nyctinastic movement in legume. *J Plant Res* 116(2):151–154.
17. Marx GA (1984) Linkage relations of *tendrilled acacia* (*tac*) and *apulvinic*. *Pisum Newsl* 16:46–48.
18. Harvey DM (1979) Evaluation of an apuvinic foliar mutation in *P. sativum* L Seventieth Annual Report (John Innes Institute, Norwich, UK), p 34.
19. Chen J, et al. (2010) Control of dissected leaf morphology by a Cys(2)His(2) zinc finger transcription factor in the model legume *Medicago truncatula*. *Proc Natl Acad Sci USA* 107:10754–10759.
20. Wang H, et al. (2008) Control of compound leaf development by *FLORICAULA/LEAFY* ortholog *SINGLE LEAFLET1* in *Medicago truncatula*. *Plant Physiol* 146:1759–1772.
21. Tadege M, et al. (2008) Large-scale insertional mutagenesis using the *Tnt1* retrotransposon in the model legume *Medicago truncatula*. *Plant J* 54:335–347.
22. Rakocevic A, et al. (2009) *MERE1*, a low-copy-number copia-type retroelement in *Medicago truncatula* active during tissue culture. *Plant Physiol* 151:1250–1263.
23. Shuai B, Reynaga-Peña CG, Springer PS (2002) The lateral organ boundaries gene defines a novel, plant-specific gene family. *Plant Physiol* 129:747–761.
24. Husbands A, Bell EM, Shuai B, Smith HM, Springer PS (2007) LATERAL ORGAN BOUNDARIES defines a new family of DNA-binding transcription factors and can interact with specific bHLH proteins. *Nucleic Acids Res* 35:6663–6671.
25. Matsumura Y, Iwakawa H, Machida Y, Machida C (2009) Characterization of genes in the ASYMMETRIC LEAVES2/LATERAL ORGAN BOUNDARIES (AS2/LOB) family in *Arabidopsis thaliana*, and functional and molecular comparisons between AS2 and other family members. *Plant J* 58:525–537.
26. Majer C, Hochholdinger F (2011) Defining the boundaries: Structure and function of LOB domain proteins. *Trends Plant Sci* 16(1):47–52.
27. Luo JH, Weng L, Luo D (2006) Isolation and expression patterns of *LATERAL ORGAN BOUNDARIES-like* genes in *Lotus japonicus*. *J Plant Physiol. Mol Biol* 32:202–208.
28. Bortiri E, et al. (2006) *ramosa2* encodes a LATERAL ORGAN BOUNDARY domain protein that determines the fate of stem cells in branch meristems of maize. *Plant Cell* 18:574–585.
29. Vollbrecht E, Springer PS, Goh L, Buckler ES, IV, Martienssen R (2005) Architecture of floral branch systems in maize and related grasses. *Nature* 436:1119–1126.
30. Evans MM (2007) The *indeterminate gametophyte1* gene of maize encodes a LOB domain protein required for embryo Sac and leaf development. *Plant Cell* 19(1):46–62.
31. Sarala K, Sharma B (1994) Additional information on the linkage of genes *apu* and *uni* of *Pisum sativum* L. *Pisum Genet* 26:28.
32. Choi HK, et al. (2004) Estimating genome conservation between crop and model legume species. *Proc Natl Acad Sci USA* 101:15289–15294.
33. Dalmais M, et al. (2008) UTILLdb, a *Pisum sativum* in silico forward and reverse genetics tool. *Genome Biol* 9:R43.
34. Yordanov YS, Regan S, Busov V (2010) Members of the LATERAL ORGAN BOUNDARIES DOMAIN transcription factor family are involved in the regulation of secondary growth in Populus. *Plant Cell* 22:3662–3677.
35. Rubin G, Tohge T, Matsuda F, Saito K, Scheible WR (2009) Members of the LBD family of transcription factors repress anthocyanin synthesis and affect additional nitrogen responses in Arabidopsis. *Plant Cell* 21:3567–3584.
36. Peng J, et al. (2011) Regulation of compound leaf development in *Medicago truncatula* by *fused compound leaf1*, a class M *KNOX* gene. *Plant Cell* 23:3929–3943.
37. Mun JH, et al. (2006) Distribution of microsatellites in the genome of *Medicago truncatula*: A resource of genetic markers that integrate genetic and physical maps. *Genetics* 172:2541–2555.
38. Tamura K, Dudley J, Nei M, Kumar S (2007) MEGA4: Molecular Evolutionary Genetics Analysis (MEGA) software version 4.0. *Mol Biol Evol* 24:1596–1599.
39. Thompson JD, Gibson TJ, Plewniak F, Jeanmougin F, Higgins DG (1997) The CLUSTAL_X windows interface: Flexible strategies for multiple sequence alignment aided by quality analysis tools. *Nucleic Acids Res* 25:4876–4882.
40. Coen ES, et al. (1990) *floricaula*: A homeotic gene required for flower development in *antirrhinum majus*. *Cell* 63:1311–1322.
41. Karimi M, Inzé D, Depicker A (2002) GATEWAY vectors for *Agrobacterium*-mediated plant transformation. *Trends Plant Sci* 7(5):193–195.